Steady-state kinetic mechanism of the NADP$^+$- and NAD$^+$-dependent reactions catalysed by betaine aldehyde dehydrogenase from *Pseudomonas aeruginosa*

Roberto VELASCO-GARCÍA*, Lilian GONZÁLEZ-SEGURA† and Rosario A. MUÑOZ-CLARES†[1]

*Laboratorio de Osmorregulación, ENEP Iztacala, Universidad Nacional Autónoma de México, Avenida de los Barrios s/n, Tlalnepantla, Estado de México, C. P. 54090, México, and †Departamento de Bioquímica, Facultad de Química, Universidad Nacional Autónoma de México, D. F. 04510, México

Betaine aldehyde dehydrogenase (BADH) catalyses the irreversible oxidation of betaine aldehyde to glycine betaine with the concomitant reduction of NAD(P)$^+$ to NADP(H). In *Pseudomonas aeruginosa* this reaction is a compulsory step in the assimilation of carbon and nitrogen when bacteria are growing in choline or choline precursors. The kinetic mechanisms of the NAD$^+$- and NADP$^+$-dependent reactions were examined by steady-state kinetic methods and by dinucleotide binding experiments. The double-reciprocal patterns obtained for initial velocity with NAD(P)$^+$ and for product and dead-end inhibition establish that both mechanisms are steady-state random. However, quantitative analysis of the inhibitions, and comparison with binding data, suggest a preferred route of addition of substrates and release of products in which NAD(P)$^+$ binds first and NAD(P)H leaves last, particularly in the NADP$^+$-dependent reaction. Abortive binding of the dinucleotides, or their analogue ADP, in the betaine aldehyde site was inferred from total substrate inhibition by the dinucleotides, and parabolic inhibition by NADH and ADP. A weak partial uncompetitive substrate inhibition by the aldehyde was observed only in the NADP$^+$-dependent reaction. The kinetics of *P. aeruginosa* BADH is very similar to that of glucose-6-phosphate dehydrogenase, suggesting that both enzymes fulfil a similar amphibolic metabolic role when the bacteria grow in choline and when they grow in glucose.

Key words: amphibolic role, parabolic inhibition, random mechanism, substrate inhibition.

INTRODUCTION

Betaine aldehyde dehydrogenase (BADH, EC 1.2.1.8) catalyses the irreversible oxidation of betaine aldehyde to glycine betaine with the concomitant reduction of NAD(P)$^+$ to NADP(H). This reaction is the final step in the biosynthesis of the osmoprotectant glycine betaine from choline [1] that takes place in response to osmotic stress in a wide variety of organisms [2–7]. In certain bacteria, such as *Escherichia coli*, glycine betaine is a non-metabolizable osmolite [7]. In contrast, in micro-organisms such as *Pseudomonas aeruginosa* [8], *Xanthomonas translucens* [9] and *Sinorhizobium meliloti* [10,11], which are able to catabolize glycine betaine, the BADH reaction is a compulsory step in the catabolism of choline or choline precursors such as phosphatidylcholine, phosphocholine, acetylcholine or choline. It is interesting that these precursors are very abundant in the infection sites of *P. aeruginosa* [12–16]. Osmotic stress conditions are also frequently present in these sites [17], and it is known that *P. aeruginosa* is able to grow under osmotic stress in the presence of the osmoprotectant glycine betaine or glycine betaine precursors [12,13]. The virulence of *P. aeruginosa* has been related to the bacterium's ability to adapt to osmotic stress [18] and to its expression of phospholipase C [19], the first enzyme in the metabolic pathway of phosphatidylcholine to glycine betaine. BADH activity therefore seems to be crucial for bacterial growth under the conditions of infection, i.e. osmotic stress plus an abundance of choline or choline precursors, and consequently to be a suitable target for antimicrobial agents. Inhibition of this enzymic activity would not only starve bacteria grown in choline or choline precursors, and/or seriously affect their ability to stand osmotic stress, but it also would stop growth, even if glycine betaine were present, owing to the toxic effect of the build-up of betaine aldehyde, as Sage et al. [20] have found in a *P. aeruginosa* mutant deficient in BADH activity.

Most of the BADH forms studied so far show a marked preference for NAD$^+$ over NADP$^+$ [3,5,21–25], with the exception of the catabolic BADH from *P. aeruginosa* [8,26] and *X. translucens* [9], which can use NADP$^+$ and NAD$^+$ as coenzymes. It is therefore likely that when the opportunistic human pathogen *P. aeruginosa* grows in choline or choline precursors as the only carbon, nitrogen and energy source, BADH behaves as a dual dehydrogenase, serving either catabolic or anabolic roles depending on whether it uses NAD$^+$ or NADP$^+$.

Kinetic studies on the *Pseudomonas* BADH are scarce and the kinetic mechanism of this important enzyme has not yet been elucidated. The kinetic mechanisms of the BADH from the fungus *Cylindrocarpon didymum* [21] and from *E. coli* [22] have been reported to be Ping Pong, and those of the enzyme from the plant *Amaranthus hypochondriacus* [27] and pig kidney [25] Iso Ordered Bi Bi steady-state. Because a complete knowledge of the kinetic mechanism of *P. aeruginosa* BADH is important to further the understanding of the possible role of the enzyme in the metabolism of choline and choline precursors in this important pathogen, and for future efforts on specific inhibitor design, we undertook the detailed characterization of the steady-state kinetics of the NADP$^+$- and NAD$^+$-dependent reactions

Abbreviation used: BADH, betaine aldehyde dehydrogenase.

[1] To whom correspondence should be addressed (e-mail clares@servidor.unam.mx).

catalysed by BADH from *P. aeruginosa*. Here we report a steady-state random kinetic mechanism with a preferred route of addition of substrates and release of products in which the oxidized dinucleotide binds first and the reduced dinucleotide leaves last. The *P. aeruginosa* BADH kinetics are fully compatible with an amphibolic metabolic role for this enzyme.

MATERIALS AND METHODS

Chemicals and biochemicals

Betaine aldehyde chloride, glycine betaine (inner salt), choline chloride, benzaldehyde, $NAD(P)^+$, NAD(P)H, dithiothreitol and 2-mercaptoethanol were obtained from Sigma (St Louis, MO, U.S.A.). All other chemicals of analytical grade were from standard suppliers.

Enzyme purification and assay

BADH was purified to homogeneity from *P. aeruginosa* PAO1 strain as described previously [26]. The enzyme does not contain $NAD(P)^+$ or NAD(P)H bound as judged by the ratio of A_{280} to A_{260}, which was 1.95. The specific activity of the enzyme preparation used, determined in a standard assay in the presence of 1.0 mM betaine aldehyde and 0.3 mM $NADP^+$ in a 100 mM potassium phosphate buffer, pH 8.0, at 30 °C, was 79 units/mg of protein. One unit of activity is defined as the amount of enzyme catalysing the formation of 1 μmol of NAD(P)H/min in our standard assay.

Kinetic studies

Steady-state initial velocity studies were performed, at 30 °C in cuvettes with a path length of 1.0 cm, in a final volume of 0.5 ml of 100 mM potassium phosphate buffer, pH 8.0, containing 1 mM EDTA at the concentrations of substrates and products stated in each experiment. The production of NAD(P)H was monitored spectrophotometrically at 340 nm (ε 6.22 $mM^{-1} \cdot cm^{-1}$) with a Philips PU 8710 spectrophotometer equipped with a kinetics software package. All assays were initiated by the addition of the enzyme (3.7 nM). Initial steady-state rates were determined from the initial, linear portions of reaction progress curves. Each point shown in the figures is the average of duplicate or triplicate determinations. In all experiments the reported aldehyde concentrations are the sum of the free and hydrated species present. Initial velocity patterns in the absence of added inhibitors were obtained by varying the concentration of the dinucleotide at several fixed levels of betaine aldehyde in the assay described above. Dead-end inhibition patterns were obtained by varying one reactant with the second fixed at a value near K_m and at different fixed levels of the inhibitor. Kinetic data were analysed by non-linear regression calculations with a commercial computing program formulated with the algorithm of Marquardt [28]. Initial velocity data in the absence of products or dead-end inhibitors at several concentrations of the fixed substrate were first individually fitted to the Michaelis–Menten equation:

$$v = V[S]/(K_m + [S]) \quad (1)$$

where v is the experimentally determined initial velocity, V is the maximal velocity, [S] is the concentration of the variable substrate and K_m is the concentration of substrate at half-maximal velocity. On the basis of the corresponding double-reciprocal plots, the mechanism was identified and the data set was fitted globally to the initial velocity equation for a sequential mechanism:

$$v = V[A][B]/(K_{ia}K_b + K_b[A] + K_a[B] + [A][B]) \quad (2)$$

where A is $NAD(P)^+$ and B is betaine aldehyde, K_a and K_b are the Michaelis–Menten constants for $NAD(P)^+$ and betaine aldehyde respectively, and K_{ia} is the dissociation constant of E–$NAD(P)^+$ (nomenclature of Cleland [29]). The analogous constant K_{ib} for the dissociation of betaine aldehyde from E–betaine aldehyde was estimated by considering that A was betaine aldehyde and B was $NAD(P)^+$, or from

$$K_{ia}K_b = K_aK_{ib} \quad (3)$$

assuming rapid equilibrium conditions. Initial velocity data for product, dead-end and substrate inhibition were first plotted as double-reciprocal plots. The form of inhibition was determined graphically by replots of intercepts and slopes. The data were globally fitted to eqn (4) or (5), corresponding to linear competitive or mixed inhibition respectively, or to eqn (6) or (7), corresponding to S-parabolic I-linear mixed or parabolic mixed inhibition respectively:

$$v = V[S]/(K_m(1 + [I]/K_{ic}) + [S]) \quad (4)$$

$$v = V[S]/\{K_m(1 + [I]/K_{ic}) + [S](1 + [I]/K_{iu})\} \quad (5)$$

$$v = V[S]/\{K_m(1 + [I]/K_{ic} + [I]^2/K_{ic}K'_{ic}) + [S](1 + [I]/K_{iu})\} \quad (6)$$

$$v = V[S]/\{K_m(1 + [I]/K_{ic} + [I]^2/K_{ic}K'_{ic}) + [S](1 + [I]/K_{iu}) + [I]^2/K_{iu}K'_{iu})\} \quad (7)$$

In these equations K_{ic} and K_{iu} are competitive and uncompetitive inhibition constants respectively of the first molecule of inhibitor bound to the enzyme, and K'_{ic} and K'_{iu} are the competitive and uncompetitive inhibition constants respectively of the second molecule of inhibitor. All other terms are as defined above. For mixed inhibition the differences between K_{ic} and K_{iu} were always less than 10-fold and more than 1.5-fold. If this difference was less than 1.5-fold the equation for non-competitive inhibition ($K_i = K_{ic} = K_{iu}$) was used.

Eqns (8) and (9) were used for total or partial substrate inhibition respectively:

$$v = V[S]/\{K_m + [S](1 + [S]/K_{IS})\} \quad (8)$$

$$v = V[S](1 + \beta[S]/K_{IS})/\{K_m + [S](1 + [S]/K_{IS})\} \quad (9)$$

where K_{IS} is the substrate inhibition constant, and β is the interaction factor that describes the effect of substrate inhibition on V.

The points in the figures are the experimentally determined values, whereas the curves are calculated from fits of these data to the appropriate equation. The best fits were determined by the relative fit error, the error of the constants and the absence of significant correlation between the residuals and other relevant variables such as observed velocities, substrate concentration and number of results.

Equilibrium dissociation constants of $NAD(P)^+$

Dissociation constants for the interaction of dinucleotides with enzyme were determined by following the quenching of intrinsic protein fluorescence. The measurements were performed at 30 °C on an LS50B luminescence spectrophotometer with a thermostatically controlled compartment (Perkin Elmer, Norwalk, CT, U.S.A.). Freshly desalted protein, in 10 mM potassium phosphate buffer, pH 8.0, containing 10 mM 2-mercaptoethanol, 0.1 mM EDTA, 20 % (w/v) sucrose and 25 mM KCl, was excited at 296 nm (5 nm bandwidth) and the emission was recorded at 333 nm (10 nm bandwidth). The enzyme concentration was 0.8 μM, which was low enough to avoid inner-filter effects of the protein. In addition, to minimize the inner-filter effects of the dinucleotides we used a microcell of path length

5 mm placed eccentrically in the cell compartment [30]. Inner-filter effects caused by NAD(P)$^+$ at 296 and 333 nm were corrected by the formula [31]:

$$F_c = F_{obs} \times 10^{[(A_{ex}+A_{em})/2]} \quad (10)$$

where F_c is the corrected intensity, F_{obs} is the measured intensity and A_{ex} and A_{em} are the absorbances at the excitation and emission wavelengths respectively. NAD(P)$^+$ titrations were performed by sequentially adding aliquots of stock solutions of the dinucleotides to a single sample of BADH in a fluorescence cuvette. The solutions were equilibrated for 2 min after each addition before the fluorescence was read. The fluorescence data were corrected for background fluorescence, for dilution of the sample and for inner-filter effects. The corrected fluorescence intensities were used to calculate the dissociation constant of the dinucleotides by fitting the data to the following equation:

$$\Delta F = \Delta F_{max}\,[NAD(P)^+]_{free}/(K_d + [NAD(P)^+]_{free}) \quad (11)$$

where ΔF is the difference between the fluorescence intensities of protein in the absence and in the presence of the dinucleotides, ΔF_{max} is this difference when all the binding sites of the enzyme are saturated with ligand and K_d is the dissociation constant of NAD(P)$^+$ from the complexes E–NAD(P)$^+$. The concentration of free ligand was estimated from $[ligand]_{free} = [ligand]_t - n[E]_t$, in which $[ligand]_t$ and $[E]_t$ represent the total concentration of ligand and the concentration of free enzyme respectively and n is the number of ligand-binding sites on the enzyme ($n = 1$ for monomer concentration). The results were expressed as percentages of the initial fluorescence.

RESULTS

Initial velocity patterns

The NADP$^+$- and NAD$^+$-dependent oxidation of betaine aldehyde followed hyperbolic saturation curves and gave linear double-reciprocal plots in the range 100–1000 μM betaine aldehyde and 25–500 μM NAD(P)$^+$ (Figure 1). The families of lines obtained intersected to the left of the $1/v$ axis, indicating a sequential kinetic mechanism. Data for the NADP$^+$-dependent reaction gave a good global fit to the equation for an ordered or rapid-equilibrium random Bi Bi mechanism [eqn (2)] (Figure 1A), whereas data for the NAD$^+$-dependent reaction gave a poorer fit as indicated by a clear deviation of the experimental points corresponding to the lowest NAD$^+$ concentrations from the theoretical line derived from the fit (Figure 1B, solid lines). In fact, when data in each line of Figure 1(B) were individually fitted by linear regression (Figure 1B, broken lines) they did not intersect in a common point. These results suggest randomness in the NAD$^+$-dependent reaction. The kinetic parameters estimated for both reactions by a global fit of the initial velocity data to eqn (2) are given in Table 1. K_i values for the dinucleotide or betaine aldehyde were estimated by considering that the dinucleotide or the aldehyde combined first with the enzyme, or assuming a rapid equilibrium random mechanism. The k_{cat} value was estimated by assuming that the enzyme is a homodimer of 109 kDa with two active sites [26].

Product inhibition patterns

To test the kinetic mechanism further, we performed inhibition studies with both products of the reaction, the reduced dinucleotides and glycine betaine. At a fixed subsaturating concentration of betaine aldehyde (0.5 mM), the inhibition by NADPH was linear competitive with respect to NADP$^+$. With betaine aldehyde as the variable substrate, at a fixed subsaturating concentration of NADP$^+$ (100 μM), NADPH was a linear mixed type inhibitor. Inhibition by NADH was more complex. Data in the inhibition pattern against NAD$^+$ were best fitted to eqn (6), corresponding to S-parabolic I-linear non-competitive inhibition (Figure 2A), whereas those in the inhibition pattern against betaine aldehyde were best fitted to eqn (7), corresponding to parabolic non-competitive inhibition, in which both slopes and intersects were a parabolic function of the concentration of the inhibitor (Figure

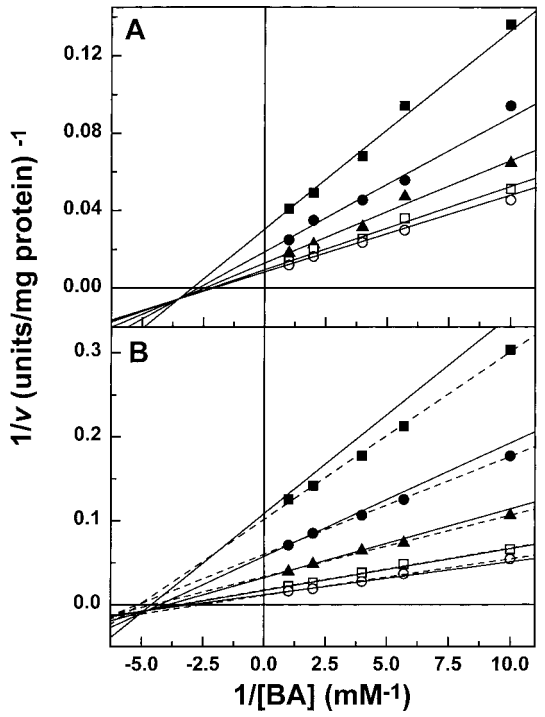

Figure 1 Initial velocity patterns of the reaction of *P. aeruginosa* BADH

Betaine aldehyde was varied in the range 0.1–1 mM at the following fixed concentrations of NADP$^+$ (**A**) or NAD$^+$ (**B**): 25 (■), 50 (●), 100 (▲), 250 (□) and 500 (○) μM. Assays were performed under the standard conditions described in the Materials and methods section. In the double-reciprocal plots the points are the experimentally determined values; the lines drawn through these points are those calculated from the best global fit to these data by non-linear regression to eqn (2). In (**B**) the broken lines are from individual linear regression fits of the data in each saturation curve.

Table 1 Kinetic parameters of the NADP$^+$- and NAD$^+$-dependent BADH from *P. aeruginosa*

Initial velocities were obtained in potassium phosphate buffer at 30 °C, pH 8.0, under the conditions described in the Materials and methods section. Results are shown as means ± S.E.M. and were estimated by a fit of the initial velocity data in Figure 1 to eqn (2).

Parameter	NADP$^+$	NAD$^+$
V (units/mg of protein)	143.0 ± 6.1	151.9 ± 7.8
K_{cat} (s^{-1})	261.0 ± 11.1	276.5 ± 14.2
$K_i^{dinucleotide}$ (μM)	47.7 ± 7.7	185.6 ± 35.1
$K_m^{dinucleotide}$ (μM)	83.4 ± 8.8	385.2 ± 42.7
$K_i^{betaine\ aldehyde}$ (μM)	289.6 ± 55.7	209.2 ± 41.4
$K_m^{betaine\ aldehyde}$ (μM)	506.8 ± 43.1	434.5 ± 44.5
$k_{cat}/K_m^{dinucleotide}$ ($M^{-1} \cdot s^{-1}$)	1.6×10^6	3.6×10^5
$k_{cat}/K_m^{betaine\ aldehyde}$ ($M^{-1} \cdot s^{-1}$)	2.6×10^5	3.1×10^5

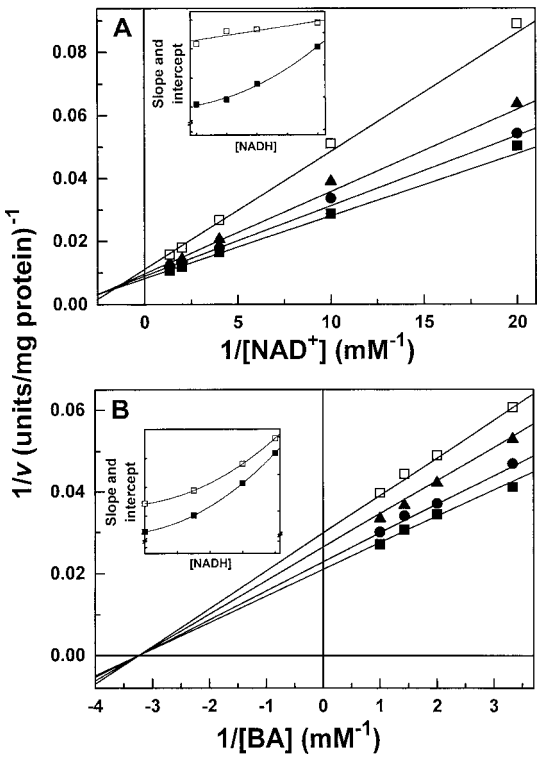

Figure 2 NADH inhibition patterns of the NAD$^+$-dependent *P. aeruginosa* BADH

(**A**) Betaine aldehyde was held at a non-saturating concentration of 1 mM; NAD^+ was varied in the range 50 μM to 1 mM at the following fixed concentrations of NADH: 0 (■), 100 (●), 200 (▲) and 400 (□) μM. (**B**) NAD^+ was fixed at 200 μM; betaine aldehyde was varied in the range 0.2–1 mM at the following fixed concentrations of NADH: 0 (■), 150 (●), 300 (▲) and 400 (□) μM. Assays were performed under the standard conditions described the Materials and methods section. In the double-reciprocal plots the points are the experimentally determined values; the lines drawn through these points are those calculated from the best non-linear regression fit of these data to eqn (6) (**A**) or to eqn (7) (**B**). Insets: replots of slopes (■) and intercepts (□) from the main figures against NADH concentration.

2B). The patterns of inhibition and inhibition constants estimated for the reduced dinucleotides are given in Table 2.

The acid product of the reaction, glycine betaine, was a very poor inhibitor. Significant inhibition was observed only at very high concentrations (50 mM and above). Glycine betaine in the concentration range 50–200 mM behaved as a linear mixed or non-competitive inhibitor with regard to either dinucleotide or betaine aldehyde. It is interesting that the estimated inhibition constants for the acid product were three orders of magnitude greater than those for the other reaction product, the reduced dinucleotide (Table 2).

Dead-end inhibition patterns

The use of dead-end inhibitors is a powerful tool to determine or confirm a kinetic mechanism [32]. In this study we used ADP as a dead-end analogue of the dinucleotides, and choline and benzaldehyde as dead-end analogues of betaine aldehyde. The use of benzaldehyde as a dead-end inhibitor was justified by initial velocity studies that showed that it was not a substrate of the *P. aeruginosa* BADH. Results of the dead-end inhibition studies are summarized in Table 3.

With $NADP^+$ as the variable substrate at a fixed subsaturating concentration of betaine aldehyde (500 μM), ADP in the concentration range 1.25–3.75 mM gave a linear competitive inhibition pattern, whereas with NAD^+ it gave an S-parabolic I-linear non-competitive inhibition pattern. However, parabolic inhibition of ADP was also observed in the $NADP^+$-dependent reaction when a wider concentration range of the inhibitor (1–15 mM) was tested (Figure 3). Interestingly, the Dixon plots of $1/v$ against ADP concentration become almost linear at a high concentration of betaine aldehyde in both the NAD^+- and $NADP^+$-dependent reactions, suggesting that binding of the second molecule of the nucleotide was competitive with the aldehyde. ADP behaved as a non-competitive inhibitor against betaine aldehyde in the $NADP^+$-dependent reaction, and as a mixed inhibitor in the NAD^+-dependent reaction. This inhibition by ADP was slope-parabolic in both cases, whereas it was intercept-linear in the $NADP^+$-dependent reaction and intercept-parabolic in the NAD^+-dependent reaction (Table 3).

Choline yielded linear mixed inhibition against $NADP^+$ and NAD^+, and linear competitive inhibition against betaine aldehyde. Benzaldehyde was tested only in the $NADP^+$-dependent reaction; its inhibition pattern against $NADP^+$ was qualitatively similar to that of choline. Quantitatively, benzaldehyde was a much more effective inhibitor than choline, as indicated for their respective K_i values, given in Table 3. This result indicates the importance of the aldehyde group for substrate binding.

Substrate inhibition

In both the NAD^+- and $NADP^+$-dependent reactions, substrate inhibition by the dinucleotide was observed (Figure 4A). At

Table 2 Product inhibition patterns and inhibition constants for the NADP$^+$- and NAD$^+$-dependent BADH from *P. aeruginosa*

Initial velocities were obtained as described in the Materials and methods section, in potassium phosphate buffer, pH 8.0, 30 °C. Initial velocity data were globally fitted to the equation for competitive (C), mixed (MX), non-competitive (NC), S-parabolic I-linear noncompetitive (S_P I_L NC) and ($_P$NC) parabolic non-competitive inhibition. Values given are means ± S.E.M. Abbreviation: BA, betaine aldehyde; GB, glycine betaine.

Variable substrate	Fixed substrate	Product	Pattern	K_{ic} (μM)	K'_{ic} (μM)	K_{iu} (μM)	K'_{iu} (μM)
$NADP^+$	BA (0.5 mM)	NADPH	C	182 ± 10			
BA	$NADP^+$ (0.1 mM)	NADPH	MX	384 ± 39		675 ± 79	
$NADP^+$	BA (0.175 mM)	GB	MX	(742 ± 408) × 10^3		(278 ± 42) × 10^3	
BA	$NADP^+$ (0.1 mM)	GB	NC	(495 ± 50) × 10^3			(495 ± 50) × 10^3
NAD^+	BA (1.0 mM)	NADH	S_P I_L NC	1075 ± 179	287 ± 152	1075 ± 179	
BA	NAD^+ (0.2 mM)	NADH	$_P$NC	3424 ± 1960	153 ± 122	3424 ± 1960	
NAD^+	BA (0.15 mM)	GB	NC	(482 ± 21) × 10^3			(482 ± 21) × 10^3
BA	NAD^+ (0.5 mM)	GB	MX	(325 ± 35) × 10^3			(547 ± 100) × 10^3

Table 3 Dead-end inhibition patterns and inhibition constants for $NADP^+$- and NAD^+-dependent BADH from *P. aeruginosa*

Initial velocities were obtained as described in the Materials and methods section, in potassium phosphate buffer, pH 8.0, 30 °C. Initial velocity data were globally fitted to the equation for competitive (C), S-parabolic I-linear noncompetitive ($S\text{-}_P\ I\text{-}_L$ NC), mixed (MX) and parabolic mixed inhibition ($_P$MX). Values given are means ± S.E.M. Abbreviation: BA, betaine aldehyde.

Variable substrate	Fixed substrate	Inhibitor	Pattern	K_{ic} (mM)	K'_{ic} (mM)	K_{iu} (mM)	K'_{iu} (mM)
$NADP^+$	BA (0.5 mM)	ADP	C	3.3 ± 0.2			
BA	$NADP^+$ (0.1 mM)	ADP	$S\text{-}_P\ I\text{-}_L$ NC	6.3 ± 0.8	9.1 ± 4.3	6.3 ± 0.8	
$NADP^+$	BA (0.5 mM)	Choline	MX	135.5 ± 20.4		49.6 ± 5.7	
BA	$NADP^+$ (0.1 mM)	Choline	C	26.4 ± 2.5			
$NADP^+$	BA (0.5 mM)	Benzaldehyde	MX	0.17 ± 0.03		0.074 ± 0.004	
NAD^+	BA (0.5 mM)	ADP	$S\text{-}_P\ I\text{-}_L$ NC	8.9 ± 0.2	5.6 ± 5.1	8.9 ± 0.2	
BA	NAD^+ (0.5 mM)	ADP	$_P$MX	9.3 ± 4.2	5.2 ± 4.5	26.4 ± 20.7	3.7 ± 4.8
NAD^+	BA (0.5 mM)	Choline	MX	108.5 ± 17.2		40.4 ± 3.2	
BA	NAD^+ (0.5 mM)	Choline	C	18.1 ± 1.0			

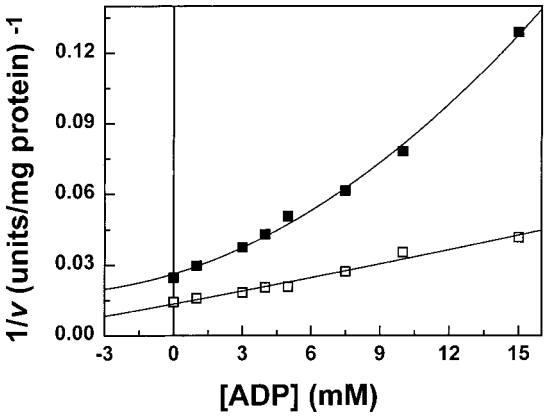

Figure 3 Inhibition of *P. aeruginosa* BADH by ADP

The concentration of $NADP^+$ was 100 μM and that of betaine aldehyde 250 μM (■) or 2.5 mM (□). The points are the experimentally determined values; the lines drawn through these points are those calculated from the best non-linear regression fit of these data to the equation of a parabola.

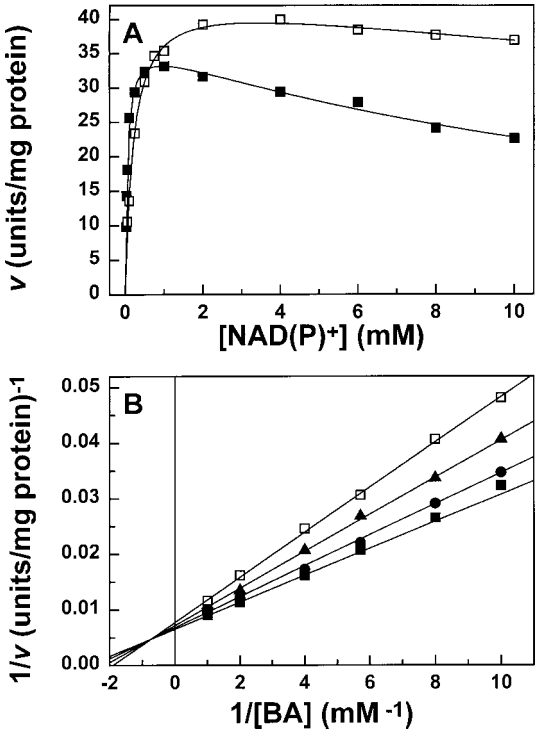

Figure 4 Substrate inhibition of the *P. aeruginosa* BADH by $NAD(P)^+$

(**A**) Betaine aldehyde was 200 μM and $NADP^+$ (□) or NAD^+ (■) were varied as indicated. (**B**) Betaine aldehyde was varied in the range from 0.1–1 mM at the following fixed, inhibitory, concentrations of $NADP^+$: 1 (■), 3 (●), 6 (▲) and 10 (□) mM. Assays were performed under the standard conditions described in the Materials and methods section. The points are the experimentally determined values; the lines drawn through these points are those calculated from the best non-linear regression fit of the data to eqn (8) (**A**) or to eqn (5) (**B**).

0.2 mM betaine aldehyde the substrate inhibition constants (means ± S.E.M.) for NAD^+ and $NADP^+$, estimated from a fit of the data to eqn (8), were 49.7 ± 7.7 and 16.1 ± 1.8 mM respectively. To gain insight into the mechanism of this inhibition, we performed initial velocity experiments in which the concentration of betaine aldehyde was varied from 0.1 to 1 mM, at several fixed, high, $NADP^+$ concentrations that were saturating in its role as substrate (1–10 mM). We found a total mixed inhibition of $NADP^+$ with regard to betaine aldehyde (Figure 4B), with a K_{ic} of 12.3 ± 1.3 mM and a K_{iu} of 48.0 ± 10.8 mM.

As reported previously [26], the $NADP^+$-dependent reaction catalysed by BADH from *P. aeruginosa* is partly inhibited by high concentrations of the aldehyde substrate. Substrate inhibition by the aldehyde is very weak, which makes it difficult to establish the mechanism. The pattern of inhibition of betaine aldehyde against $NADP^+$ seems to be consistent with uncompetitive partial inhibition, which is suggestive of the formation of the non-productive ternary complex E–NADPH–betaine aldehyde, from which NADPH can be released. We did not observe inhibition by betaine aldehyde in the NAD^+-dependent reaction, even when the aldehyde concentration was increased to 60 mM.

Dissociation constant of enzyme–$NAD(P)^+$ complexes

The binding of $NAD(P)^+$ quenches the intrinsic protein fluorescence of the enzyme [26]. The value of the dissociation constant (K_d) for $NAD(P)^+$ binding can be determined from the dependence of fluorescence intensity on dinucleotide concentration. Both nucleotides seem to induce similar conformational changes on binding to the enzyme, although the binding of NAD^+ produces a greater quenching response than $NADP^+$ in enzyme fluorescence. Thus the maximum fluorescence change caused by

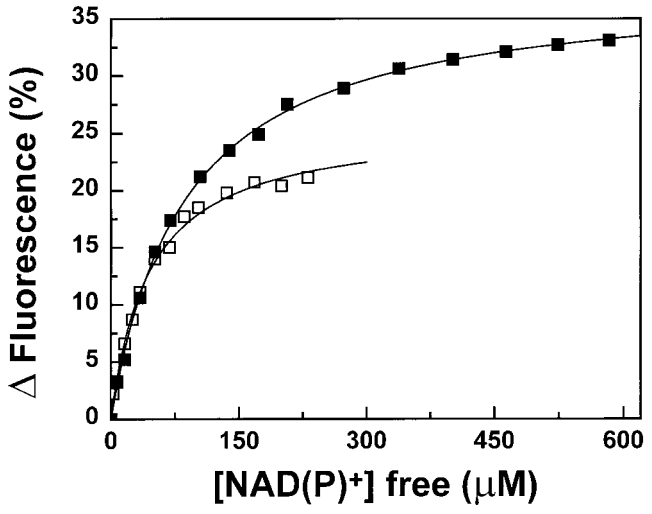

Figure 5 Binding of the oxidized dinucleotides to *P. aeruginosa* BADH

Dependence of the fractional saturation of the enzyme, as measured from the quenching of intrinsic fluorescence, on the concentration of $NADP^+$ (□) or NAD^+(■). The enzyme concentration was 0.8 μM. The data were fitted to eqn (11).

NAD^+ was 38 %, whereas $NADP^+$ caused a change of 26 %. The binding curves were hyperbolic (Figure 5) and the data gave a good fit to eqn (11) with K_d values of 45.3 ± 3.1 and 85.4 ± 2.4 μM for $NADP^+$ and NAD^+ respectively.

DISCUSSION

Kinetic mechanism

BADH catalyses an irreversible reaction; kinetic analysis is therefore limited to initial-velocity studies of the forward reaction in the absence and in the presence of inhibitors. Neither the reverse reaction nor isotopic exchange between products and substrates can be demonstrated. Moreover, the accuracy of the kinetic parameters cannot be tested by the Haldane relationships.

The initial velocity patterns obtained in the $NADP^+$-dependent reaction are consistent with a sequential mechanism, either steady-state ordered or rapid equilibrium random [29], whereas in the NAD^+-dependent reaction the experimental points do not fit well with the velocity equation for these mechanisms. However, patterns of inhibition by the acid product of the reaction, glycine betaine, were similar in both reactions and suggested of steady-state mechanisms with a random release of products. Ordered mechanisms are ruled out because, given the irreversibility of the BADH-catalysed reaction, glycine betaine would be an uncompetitive inhibitor against both dinucleotides and against betaine aldehyde if $NAD(P)^+$ was added first to the enzyme and NAD(P)H was released last, or competitive against the aldehyde and non-competitive against the dinucleotide if betaine aldehyde was the first substrate and glycine betaine was the last product. Glycine betaine, at the very high concentrations required to inhibit the enzyme, might also form dead-end complexes E–$NAD(P)^+$–glycine betaine, which would result in slope effects of glycine betaine on the kinetics of saturation by betaine aldehyde, and intercept effects in those of the dinucleotide. However, if these effects do exist they would add to those originating from the formation of the non-productive complexes E–glycine betaine and E–NAD(P)H–glycine betaine, so the same inhibition patterns would be observed.

Even if the release of products is random, the affinity of free enzyme for glycine betaine is so low (Table 2) that it can be safely concluded that under normal conditions *in vivo* and *in vitro* there are no kinetically significant levels of the binary complex E–glycine betaine, so the added reduced dinucleotides can bind only to free enzyme. Moreover, because NADH and NADPH cannot reverse the reaction flux, they could be considered to be dead-end analogues of the oxidized dinucleotides. Therefore the inhibition patterns of the reduced dinucleotides will be interpreted within this framework. Data for dead-end inhibition (Table 3) point to a steady-state random addition of substrates, because ADP, choline and benzaldehyde are mixed inhibitors against the substrate for which they are not analogues. Product inhibition patterns by NAD(P)H are also consistent with a random addition of substrates, although that of NADH against NAD^+ is more complex and will be discussed below.

The initial velocity patterns in a steady-state random mechanism may seem linear depending on the values of the 'off' constants for the substrates from the complexes with the enzyme relative to k_{cat} [33]. These patterns can be fitted to the equation for a rapid equilibrium random mechanism [eqn (2)] but this fit will give incorrect values of the dissociation constants. The quantitative validity of the K_i^{NADP} and $K_i^{betaine\ aldehyde}$ values, estimated from a fit of the initial velocity data of the $NADP^+$-dependent reaction to eqn (2) assuming either the rapid equilibrium random addition of substrates or the ordered mechanisms in which the first substrate was $NADP^+$ or betaine aldehyde, was ascertained from a calculation of the true dissociation constants of $NAD(P)^+$ and betaine aldehyde from their binary complexes with free enzyme. The K_d of the E–$NADP^+$ complex is in excellent agreement with the initial velocity determined value, whereas that of E–NAD^+ is approx. one half the K_i^{NAD+}. The K_d of the E–betaine aldehyde complex, determined by taking advantage of the protection afforded by the aldehyde against inactivation of the enzyme by chemical modification (L. González-Segura and R. A. Muñoz-Clares, unpublished work), was 1.35 ± 0.07 mM, which is more than 5-fold that for $K_i^{betaine\ aldehyde}$ calculated from the initial velocity patterns (Table 1). The latter result rules out both a random rapid equilibrium or an ordered mechanism with betaine aldehyde binding first. In the $NADP^+$-dependent reaction, the mechanism seems to be predominantly ordered, with $NADP^+$ combining with the enzyme first, at least in the substrate concentration range used in our studies, which we expect to be not far from the physiological range. In the NAD^+-dependent reaction, our data support a random steady-state kinetic mechanism, although the reaction pathway in which the dinucleotide binds first might still be the preferred one. These differences between the reactions with both dinucleotides might be due to the lower affinity of the free enzyme for NAD^+ than for $NADP^+$, which under identical conditions would result in higher steady-state levels of the complex E–betaine aldehyde in the NAD^+-dependent reaction. In addition, it is possible that NAD^+ binds better than $NADP^+$ to the latter complex, as suggested by the lack of substrate inhibition by the aldehyde in the NAD^+-dependent reaction.

In ordered or rapid equilibrium random mechanisms, K_b is the true dissociation constant of B from the E–A–B complex. This definition is also reasonably valid for steady-state random mechanisms [33]. Thus we can compare the K_m for betaine aldehyde estimated from the initial velocity patterns in the $NADP^+$- and NAD^+-dependent reactions with the dissociation constant of betaine aldehyde from the E–betaine aldehyde complex determined by chemical modification. From these comparisons it seems that betaine aldehyde has a 3-fold weaker affinity for the free enzyme than for the E–$NAD(P)^+$ complexes,

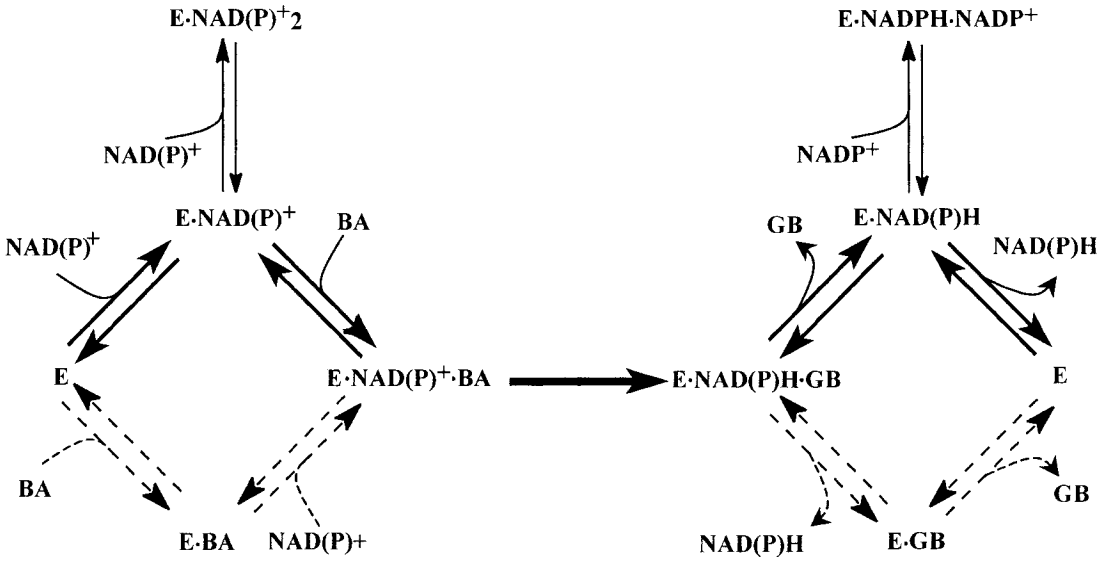

Scheme 1 Proposed kinetic mechanism for *P. aeruginosa* BADH in the absence of products

The preferred route of addition of substrates and release of products at low concentrations of substrates is shown by solid arrows.

which is consistent with the proposed preferred order of binding of substrates. The same conclusion applies to betaine analogues, as can be deduced from the inhibition constants given in Table 3.

Product inhibition patterns by NADPH against $NADP^+$ and by NADH against NAD^+ are competitive and S-parabolic non-competitive respectively. Assuming that the reduced dinucleotides behave as dead-end inhibitors, as discussed above, NADPH inhibition patterns are consistent with either an ordered ($NADP^+$ binding first) or a random addition of substrates, because in both mechanisms saturation by $NADP^+$ overcomes inhibition by the reduced dinucleotide. However, the intercept effects of NADH against NAD^+ and betaine aldehyde are not consistent with either a random or an ordered addition of substrates. The formation of an abortive E–betaine aldehyde–NADH complex, which would account for these effects, is ruled out by the lack of inhibition by betaine aldehyde, even in the presence of added NADH (results not shown). The differences between the two reactions in the patterns of inhibition by the reduced dinucleotides are confirmed by the finding of non-competitive and competitive inhibition of ADP against NAD^+ and of ADP against $NADP^+$ respectively. Non-competitive inhibition of NADH against NAD^+ has been found previously with the enzymes from amaranth [27] and from pig kidney [25] and was considered to be evidence for iso mechanisms, in which NAD^+ and NADH bind to different forms of the free enzyme. However, an alternative and plausible explanation arises from the observed parabolic slope effects of NADH and of ADP, which indicate the consecutive addition of two nucleotide molecules to the enzyme, yielding E–$NADH_2$ and E–ADP_2 dead-end complexes. The second molecule of nucleotide might combine at the betaine-aldehyde-binding site, as suggested by the change of shape of the Dixon plot for ADP inhibition, which goes from clear parabolic at low concentrations of betaine aldehyde to almost linear at high concentrations. In this regard the structural similarity between the catalytic and coenzyme-binding domains, which is a common feature of several dehydrogenases including BADH [34–36], is interesting. It is then likely that the linear intercept effect of NADH and ADP in the saturation by NAD^+ would be the result of the ability of these nucleotides to add to the E–NAD^+ complex to give the dead-end complexes E–NAD^+–NADH and E–NAD^+–ADP respectively. When the betaine aldehyde concentration is varied, inhibition by NADH and ADP is respectively non-competitive and mixed, with parabolic slope and intercept effects, which is compatible with the formation of the abortive complexes proposed above. It is interesting that, although inhibition by ADP against $NADP^+$ seems to be linear, we observed parabolic inhibition against betaine aldehyde and parabolic Dixon plots at fixed $NADP^+$ and betaine aldehyde concentrations (Figure 3). Thus the lack of parabolic effects in the inhibition of NADPH against $NADP^+$ might be due to steady-state levels of the E–$NADP^+$–NADPH and E–$NADPH_2$ complexes that are not kinetically significant at the $NADP^+$ and NADPH concentrations used in our experiments.

The parabolic inhibition by the nucleotides is fully consistent with the substrate inhibition by $NAD(P)^+$ found in both reactions. Because the formation of the ternary abortive complex E–glycine betaine–$NAD(P)^+$ is not very likely, given that kinetically significant levels of the complex E–glycine betaine were not observed even when up to 30 mM glycine betaine was added to the reaction medium, the most probable explanation for the inhibition by $NAD(P)^+$ is the formation of the non-productive complexes E–$NAD(P)_2^+$ and E–NADPH–$NADP^+$, which would account for the observed mixed pattern of inhibition against betaine aldehyde. Thus our results from dead-end and substrate inhibition by $NAD(P)^+$ support the existence in *P. aeruginosa* BADH of two binding sites for the nucleotides, one productive and another non-productive, with very different affinities.

In summary, we propose that the simplest kinetic model that accounts for the observed initial velocity and inhibition patterns of *P. aeruginosa* BADH is a steady-state Random Bi Bi mechanism, with a preferred route of addition of substrates and release of products, particularly in the $NADP^+$-dependent reaction, which is predominantly ordered, as outlined in Scheme 1. This mechanism is quite different from that reported for other BADH forms. On the sole basis of initial velocity studies it has

been concluded that the enzymes from *C. didymum* and *E. coli* follow a Ping Pong mechanism [21,22]. However, Ping Pong mechanisms are not consistent with the chemistry of the aldehyde dehydrogenases [37] and contrast with the known sequential mechanism of aldehyde dehydrogenases [38–40]. On the basis of initial velocity, product and dead-end inhibition studies, steady-state ordered iso mechanisms have been proposed for BADH from amaranth leaves [27] and from pig kidney [25]. However, the kinetic mechanisms of BADHs might not be so different; they deserve to be re-evaluated. It is therefore interesting that the amaranth enzyme follows an apparent Ping Pong mechanism at high substrate concentrations [41] and exhibits substrate inhibition by the dinucleotide [42]. If the mechanism of this inhibition is the same as that which we are proposing for *P. aeruginosa* BADH, the mixed inhibition of NADH against NAD^+ could be accounted for by the formation of the complex E.NAD^+–NADH, as discussed above, and an iso mechanism would not be required to explain the uncompetitive effects. Substrate inhibition by the dinucleotide has also been found in glutamic γ-semialdehyde dehydrogenase from human liver [43] but the mechanism of this inhibition has not been elucidated.

Physiological implications of the kinetic mechanism

BADH from *P. aeruginosa* has a dual nucleotide specificity, which is consistent with its serving either anabolic or catabolic roles depending on whether it uses $NADP^+$ or NAD^+. On the basis of the $k_{cat}/K_m^{dinucleotide}$ values, NAD^+ was one-quarter as effective as $NADP^+$ as the coenzyme of the *P. aeruginosa* BADH reaction but the ratio of $[NAD]^+$ to $[NADP]^+$, which is supposed to be approx. 5:1 [44,45], might overcome these differences. In addition, the ratio of the two BADH activities might be regulated by the ratio of [NAD^+] to [NADH] or of [$NADP^+$] to [NADPH].

When *P. aeruginosa* grows in choline or choline precursors, BADH might fulfil an amphibolic metabolic role similar to that of glucose-6-phosphate dehydrogenase when the bacteria grow in glucose, because *P. aeruginosa* catabolizes glucose via the Entner–Doudoroff pathway [46]. If this is so, it is most likely that both enzymes would be subjected to the same mechanisms of metabolic regulation to provide the bacteria with its requirements of NAD^+ or $NADP^+$. In this regard, it is interesting that the kinetic parameters for the coenzymes and the substrates have very close values in both enzymes ([47], and the present study). The kinetic mechanism of glucose-6-phosphate dehydrogenase from *P. aeruginosa* has not yet been elucidated but it has been reported that the mechanism of the same amphibolic enzyme from *Leuconostoc mesenteroides* is ordered for the $NADP^+$-dependent reaction and random for the NAD^+-dependent [48]. Further, the inhibition patterns of the *L. mesenteroides* glucose-6-phosphate dehydrogenase by the reduced dinucleotides are also very similar to those of *P. aeruginosa* BADH. In both enzymes, NADPH is a competitive inhibitor against $NADP^+$, whereas NADH is a mixed inhibitor against NAD^+ [48]. Finally, the use of NAD^+ over $NADP^+$ in glucose-6-phosphate dehydrogenase is promoted by increasing the concentration of glucose-6-phosphate [49]. The preference of *P. aeruginosa* BADH for the coenzyme used also seems to be affected by the concentration of betaine aldehyde, although to a smaller extent, as suggested by the value of $k_{cat}/K_m^{betaine\ aldehyde}$, which is 25% higher in the NAD^+-dependent than in the $NADP^+$-dependent reaction (Table 1).

This work was supported by a grant from Consejo Nacional de Ciencia y Tecnología (CONACYT-2552P-N).

REFERENCES

1 Wyn Jones, R. G. and Storey, R. (1981) Betaines. In Physiology and Biochemistry of Drought Resistance in Plants (Paleg, L. and Aspinall, D., eds.), pp. 171–204, Academic Press, Sydney

2 Pan, S., Moreau, R. A., Yu, C. and Huang, A. H. C. (1981) Betaines accumulation and betaine-aldehyde dehydrogenase in spinach leaves. Plant Physiol. **67**, 1105–1108

3 Weretilnyk, E. A. and Hanson, A. D. (1989) Betaine aldehyde dehydrogenase from spinach leaves. Purification, *in vitro* translation of the mRNA, and regulation by salinity. Arch. Biochem. Biophys. **271**, 56–63

4 Arakawa, K., Katayama, M. and Takabe, T. (1990) Levels of betaine and betaine aldehyde dehydrogenase activity in the green leaves, and etiolated leaves and roots of barley. Plant Cell Physiol. **31**, 797–807

5 Valenzuela-Soto, E. M. and Muñoz-Clares, R. A. (1994) Purification and properties of betaine aldehyde dehydrogenase extracted from detached leaves of *Amaranthus hypochondriacus* L. subjected to water deficit. J. Plant Physiol. **143**, 145–152

6 Petronini, P. G. M., De Angelis, E., Borghetti, P., Borghetti, A. F. and Wheeler, K. P. (1992) Modulation by betaine of cellular responses to osmotic stress. Biochem. J. **282**, 69–73

7 Landalf, B. and Stroem, A. R. (1986) Choline-glycine betaine pathway confers a high level of osmotic tolerance in *Escherichia coli*. J. Bacteriol. **165**, 849–855

8 Nagasawa, T., Kawabata, Y., Tani, Y. and Ogata, K. (1976) Purification and characterization of betaine aldehyde dehydrogenase from *Pseudomonas aeruginosa*. A-16. Agric. Biol. Chem. **40**, 1743–1749

9 Mori, N., Yoshida, N. and Kitamoto, Y. (1992) Purification and properties of betaine aldehyde dehydrogenase from *Xanthomonas translucens*. J. Ferment. Bioeng. **73**, 352–356

10 Bernard, T., Perroud, B., Pocard, J. A. and Le Rudulier, D. (1986) Variations in the response of salt-stressed *Rhizobium* strains to betaines. Arch. Microbiol. **143**, 359–364

11 Smith, L. T., Pocard, J. A., Bernard, T. and Le Rudulier, D. (1988) Osmotic control of glycine betaine biosynthesis and degradation in *Rhizobium meliloti*. J. Bacteriol. **170**, 3142–3149

12 D'souza-Ault, M. R., Smith, L. T. and Smith, G. M. (1993) Roles of N-acetylglutaminyl-glutamine amide and glycine betaine in adaptation of *Pseudomonas aeruginosa* to osmotic stress. Appl. Environ. Microbiol. **59**, 473–478

13 Lisa, T. A., Casale, C. H. and Domenech, C. E. (1994) Cholinesterase, acid phosphatase, and phospholipase C of *Pseudomonas aeruginosa* under hyperosmotic conditions in a high-phosphate medium. Curr. Microbiol. **28**, 71–76

14 Rennick, B. R. (1981) Renal tubule transport of organic ions. Am. J. Physiol. **240**, F83–F89

15 Pesin, S. R. and Candia, O. A. (1982) Acetylcholine concentration and its role in ionic transport by the corneal epithelium. Invest. Ophtalmol. Vis. Sci. **22**, 651–659

16 Wrigth, J. R. and Clements, J. A. (1987) Metabolism and turnover of lung surfactant. Am. Rev. Respir. Dis. **136**, 426–444

17 Kilbourne, J. P. (1978) Bacterial content and ionic composition of sputum in cystic fibrosis. Lancet **i**, 334

18 Shortridge, V. D., Lazdunski, A. and Vasil, M. L. (1992) Osmoprotectants and phosphate regulate expression of phospholipase C in *Pseudomonas aeruginosa*. Mol. Microbiol. **6**, 863–871

19 Ostroff, R. M., Wretlind, B. and Vasil, M. L. (1990) Molecular comparison of a nonhemolytic and a hemolytic phospholipase C from *Pseudomonas aeruginosa*. J. Bacteriol. **172**, 5915–5923

20 Sage, A. E., Vasil, A. I. and Vasil, M. L. (1997) Molecular characterization of mutants affected in the osmoprotectant-dependent induction of phospholipase C in *Pseudomonas aeruginosa*. Mol. Microbiol. **23**, 43–56

21 Mori, N., Kawakami, B., Hyakutome, K., Tani, Y. and Yamada, H. (1980) Characterization of betaine aldehyde dehydrogenase from *Cylindrocarpon didymum* M-1. Agric. Biol. Chem. **40**, 3015–3016

22 Falkenberg, P. and Stroem, A. R. (1990) Purification and characterization of osmoregulatory betaine aldehyde dehydrogenase from *Escherichia coli*. Biochim. Biophys. Acta **1034**, 253–259

23 Dragolovich, J. and Pierce, S. K. (1994) Characterization of partially purified betaine aldehyde dehydrogenase from horseshoe crab (*Limulus polyphemus*) cardiac mitochondria. J. Exp. Zool. **270**, 417–425

24 Chern, M. K. and Pietruszko, R. (1995) Human aldehyde dehydrogenase E3 isozyme is a betaine aldehyde dehydrogenase. Biochem. Biophys. Res. Commun. **213**, 561–568

25 Figueroa-Soto, C. G. and Valenzuela-Soto, E. M. (2000) Kinetic study of porcine kidney betaine aldehyde dehydrogenase. Biochem. Biophys. Res. Commun. **269**, 596–603

26 Velasco-García, R., Mújica-Jiménez, C., Mendoza-Hernández, G. and Muñoz-Clares, R. A. (1999) Rapid purification and properties of betaine aldehyde from *Pseudomonas aeruginosa*. J. Bacteriol. **181**, 1292–1300

27 Valenzuela-Soto, E. M. and Muñoz-Clares, R. A. (1993) Betaine-aldehyde dehydrogenase from leaves of *Amaranthus hypochondriacus* L. exhibits an Iso Ordered Bi Bi steady state mechanism. J. Biol. Chem. **268**, 23818–23823 (additions and corrections, J. Biol. Chem. **269**, 4692)
28 Marquardt, D. W. (1963) An algorithm for least-squares estimation of nonlinear parameters. J. Soc. Ind. Appl. Math. **11**, 431–441
29 Cleland, W. W. (1963) The kinetics of enzyme-catalyzed reactions with two or more substrates or products. I. Nomenclature and rate equations. Biochim. Biophys. Biochim. Biophys. Acta **467**, 104–137
30 Chen, R. F. and Hayes, J. E. (1965) Fluorescence assay of high concentrations of DPNH and TPNH in a spectrophotofluorometer. Anal. Biochem. **1**, 523–529
31 Lakowics, J. R. (1983) Principles of Fluorescence Spectroscopy, p. 44, Plenum Press, New York
32 Cleland, W. W. (1970) Steady state kinetics. In The Enzymes, 3rd edn (Boyer, P. D. ed.), vol. 2, pp. 1–65, Academic Press, New York
33 Bar-Tana, J. and Cleland, W. W. (1974) Rabbit muscle phosphofructokinase II. Product and dead end inhibition. J. Biol. Chem. **249**, 1271–1276
34 Steinmetz, C. G., Xie, P., Weiner, H. and Hurley, T. D. (1997) Structure of mitochondrial aldehyde dehydrogenase: the genetic component of ethanol aversion. Structure **5**, 701–711
35 Kutzenko, A. S., Lamzin, V. S. and Popov, V. O. (1998) Conserved supersecondary structural motif in NAD-dependent dehydrogenases. FEBS Lett. **423**, 105–109
36 Johansson, K., El-Ahmad, M., Ramaswamy, S., Hjelmqvist, L., Jornvall, H. and Eklund, H. (1998) Structure of betaine aldehyde dehydrogenase at 2.1 Å resolution. Protein Sci. **7**, 2106–2117
37 Farrés, J., Wang, T. T. Y., Cunningham, S. J. and Weiner, H. (1995) Investigation of the active site cysteine residue of rat liver mitochondrial aldehyde dehydrogenase by site-directed mutagenesis. Biochemistry **34**, 2592–2598
38 Bradbury, S. L. and Jakoby, W. B. (1971) Ordered binding of substrates to yeast aldehyde dehydrogenase. J. Biol. Chem. **246**, 1834–1840
39 Rivett, A. J. and Tipton, K. F. (1981) Kinetic studies with rat-brain succinic-semialdehyde dehydrogenase. Eur. J. Biochem. **117**, 187–193
40 Ryzewski, C. N. and Pietruszko, R. (1980) Kinetic mechanism of horse liver alcohol dehydrogenase. Biochemistry **19**, 4843–4848
41 Vojtechová, M., Rodríguez-Sotres, R., Valenzuela-Soto, E. M. and Muñoz-Clares, R. A. (1997) Substrate inhibition by betaine aldehyde of betaine aldehyde dehydrogenase from leaves of *Amaranthus hypochondriacus* L. Biochem. Biophys. Acta **1341**, 49–57
42 Muñoz-Clares, R. A., Vojtechová, M., Mújica-Jiménez, C. and Rodríguez-Sotres, R. (1996) Effects of glycerol on the kinetic properties of betaine aldehyde dehydrogenase. Adv. Exp. Med. Biol. **414**, 261–268
43 Forte-McRobbie, C. M. and Pietruszko, R. J. (1986) Purification and characterization of human liver 'high K_m' aldehyde dehydrogenase and its identification as glutamic γ-semialdehyde dehydrogenase J. Biol. Chem. **261**, 2154–2163
44 Kaplan, N. O. (1960) The pyridine coenzymes. In The Enzymes, 2nd edn (Boyer, P. D., Lardy, H. and Myrback, K., eds) vol. 3, pp. 105–169, Academic Press, New York
45 Takebe, I. and Kitahara, H. (1963) Levels of nicotinamide nucleotide coenzymes in lactic acid bacteria. J. Gen. Appl. Microbiol. **9**, 31–40
46 Hunt, J. C. and Phibbs, Jr, P. V. (1983) Regulation of alternate peripheral pathways of glucose catabolism during aerobic and anaerobic growth of *Pseudomonas aeruginosa*. J. Bacteriol. **154**, 793–802
47 Ma, J. F., Hager, P. W., Howell, M. L., Phibbs, P. V. and Hassett, D. J. (1998) Cloning and characterization of the *Pseudomonas aeruginosa zwf* gene encoding glucose-6-phosphate dehydrogenase, an enzyme important in resistance to methyl viologen (paraquat). J. Bacteriol. **180**, 1741–1749
48 Levy, R. H., Christoff, M, Ingulli, J. and Ho, E. M. L. (1983) Glucose-6-phosphate dehydrogenase from *Leuconostoc mesenteroides*: revised kinetic mechanism and kinetics of ATP inhibition. Arch. Biochem. Biophys. **222**, 473–488
49 Levy, R. H., Daouk, G. H. and Katopes, M. A. (1979) Simultaneous analysis of NAD- and NADP-linked activities of dual nucleotide-specific dehydrogenases. Arch. Biochem. Biophys. **198**, 406–413

Received 22 May 2000/8 September 2000; accepted 5 October 2000